Fabrication of Gas Nanosensors and Microsensors via Local Anodic Oxidation

ARTICLE *in* LANGMUIR · FEBRUARY 2009

Impact Factor: 4.46 · DOI: 10.1021/la803105f · Source: PubMed

7 AUTHORS, INCLUDING:

Alem-Mar Bernardes Goncalves
Universidade Federal de Mato Grosso do Sul
13 PUBLICATIONS **153** CITATIONS
SEE PROFILE

Diego C. B. Alves
Universidade Federal de Mato Grosso do Sul
9 PUBLICATIONS **249** CITATIONS
SEE PROFILE

A.s. Ferlauto
Federal University of Minas Gerais
93 PUBLICATIONS **1,432** CITATIONS
SEE PROFILE

Bernardo R A Neves
Federal University of Minas Gerais
82 PUBLICATIONS **1,182** CITATIONS
SEE PROFILE

Langmuir

Article

Fabrication of Gas Nanosensors and Microsensors via Local Anodic Oxidation

Braulio S. Archanjo, Guilherme V. Silveira, Alem-Mar B. Goncalves, Diego C. B. Alves, Andre S. Ferlauto, Rodrigo G. Lacerda, and Bernardo R. A. Neves

Langmuir, **2009**, 25 (1), 602-605 • DOI: 10.1021/la803105f • Publication Date (Web): 11 December 2008

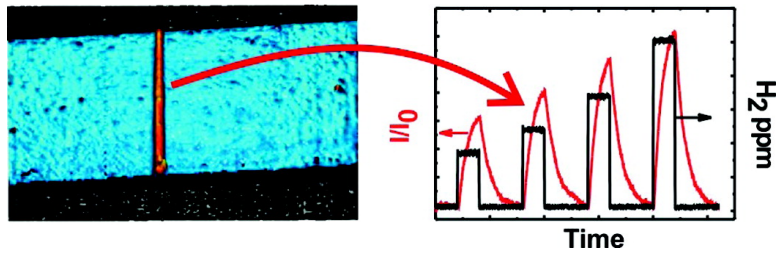

More About This Article

Additional resources and features associated with this article are available within the HTML version:

- Supporting Information
- Access to high resolution figures
- Links to articles and content related to this article
- Copyright permission to reproduce figures and/or text from this article

View the Full Text HTML

Fabrication of Gas Nanosensors and Microsensors via Local Anodic Oxidation

Braulio S. Archanjo, Guilherme V. Silveira, Alem-Mar B. Goncalves, Diego C. B. Alves, Andre S. Ferlauto, Rodrigo G. Lacerda, and Bernardo R. A. Neves*

Departamento de Física, Universidade Federal de Minas Gerais (UFMG), Avenida Antonio Carlos, 6627, Belo Horizonte, MG, Brazil

Received August 11, 2008. Revised Manuscript Received November 3, 2008

A nanosensor and microsensor fabrication method employing scanning probe microscopy (SPM) is demonstrated. Within such process, nano- or microscale metal oxide (MoO_x or TiO_x) structures, constituting the active region of a sensor, are directly fabricated onto a microscopic metal track via SPM-assisted local anodic oxidation (LAO). Two distinct LAO routes, a slow (conventional) or a fast (unusual) one, are employed to produce nano- and microsensors, which are tested at different temperatures using CO_2 and H_2 as test gases. Sensitivities down to ppm levels are demonstrated, and the possibility of easy integration into microfabrication processes is also discussed.

Introduction

Metal oxide sensors have attracted enormous attention in both industrial and scientific communities, as they are widely applicable to gas sensing, and, indeed, many commercial products can be found.[1] In most cases, the working principle of the sensor is simply based on conductivity variations when different gas species are adsorbed on its surface.[1−3] Moreover, recent advances in microfabrication techniques have opened the possibility of fabrication and integration of metal oxide sensors. A well-known example is the growth and manipulation of metal oxide nanowires and their use as gas sensors (although the need of individual nanowire manipulation prevents any large-scale application).[4−9] Recently, a new gas microsensor fabrication process has also been demonstrated, in which drops of metal oxide precursors are placed onto microgap electrodes by using a micromanipulator, dried, and calcined.[10−12] The viability of these microsensors has also been demonstrated with three different metal oxide precursors.[10−12]

The local anodic oxidation (LAO) process, based on an applied bias between the scanning probe microscopy (SPM) tip and sample, was first demonstrated in 1990, employing the scanning tunneling microscopy technique.[13] In 1993, the process was also successfully applied using atomic force microscopy (AFM),[14] and, in 1996, a single electron transistor operating at room temperature was built using the LAO process.[15] As it can be seen in the literature, since then, numerous devices have been proposed and built using the LAO process.[16−18]

This work demonstrates a new fabrication method for metal oxide nanosensors and microsensors using SPM-based LAO technique.[19] The method, which is quite simple and easily reproducible, can be summarized in two steps: the first uses conventional optical lithography to build a micron-scale, thin metallic track with macroscopic electrical contacts; and the second uses a slow (fast) LAO route to oxidize nano- (micron-) scale regions of the film, creating a metal oxide that constitutes the active region of the sensor. In order to demonstrate the viability of this methodology, two metals, Mo and Ti, are used to fabricate metal oxide (MoO_x and TiO_x, respectively) nanosensors and microsensors, which are tested, i.e., their electrical conductivities are monitored, using two distinct gases, CO_2 (oxidizing test gas) and H_2 (reducing test gas), under commercial N_2 (dry air) atmosphere at different temperatures. Therefore, the sensors' working principles, their sensitivity to each gas, influence of sensor size, temperature, and a possible integration of this methodology into a mass fabrication process are discussed.

Experimental Section

The fabrication process initiates with a conventional photolithography step, where metal (Ti or Mo) tracks, a few microns wide and hundreds of microns long, are defined on an insulating silicon dioxide substrate. During this procedure, titanium or molybdenum (99.99% purity) is deposited either by thermal evaporation or by RF sputtering, with a film thickness varying from 5 nm up to 20 nm. Macroscopic electrical contact regions are simultaneously defined at each track end in this step.

* Corresponding author. E-mail: bernardo@fisica.ufmg.br.

(1) Madou, M. J.; Morrison, S. R. *Chemical Sensing With Solid State Devices*; Academic Press: New York, 1989.
(2) Gopel, W.; Schierbaum, K. D. *Sens. Actuators, B* **1995**, *26*, 1.
(3) Barsan, N.; Weimar, U. *J. Phys.: Condens. Matter* **2003**, *15*, R813.
(4) Zhang, D.; Liu, Z.; Li, C.; Tang, T.; Liu, X.; Han, S.; Lei, B.; Zhou, C. *Nano Lett.* **2004**, *10*, 1919.
(5) Kolmakov, A.; Klenov, D. O.; Lilach, Y.; Stemmer, S.; Moskovits, M. *Nano Lett.* **2005**, *4*, 667.
(6) Sysoev, V. V.; Button, B. K.; Wepsiec, K.; Dmitriev, S.; Kolmakov, A. *Nano Lett.* **2006**, *8*, 1584.
(7) Kim, I.; Rothschild, A.; Lee, B. H.; Kim, D. Y.; Jo, S. M.; Tuller, H. L. *Nano Lett.* **2006**, *9*, 2009.
(8) Hernandez-Ramírez, F.; Rodriguez, J; Casals, O.; Russinyol, E.; Vila, A; Romano-Rodríguez, A.; Morante, J. R.; Abid, M. *Sens. Actuators, B* **2006**, *118*, 198.
(9) Modi, A.; Koratkar, N.; Lass, E.; Wei, B.; Ajayan, P. M. *Nature* **2003**, *424*, 171.
(10) Tamaki, J.; Miyaji, A.; Makinodan, J.; Ogura, S.; Konishi, S. *Sens. Actuators, B* **2005**, *108*, 202.
(11) Tamaki, J.; Niimi, J.; Ogura, S.; Konishi, S. *Sen. Actuators, B* **2006**, *117*, 353.
(12) Tamaki, J.; Nakataya, Y.; Konishi, S. *Sens. Actuators, B* **2008**, *130*, 400.
(13) Dagata, J. A.; Schneir, J.; Harary, H. H.; Evans, C. J.; Postek, M. T.; Bennett, J. *Appl. Phys. Lett.* **1990**, *56*, 2001.
(14) Day, H. C.; Alleea, D. R. *Appl. Phys. Lett.* **1993**, *62*, 2691.
(15) Matsumoto, K.; Ishii, M.; Segawa, K.; Oka, Y.; Vartanian, B. J.; Harris, J. S. *Appl. Phys. Lett.* **1996**, *68*, 34.
(16) Snow, E. S.; Campbell, P. M. *Science* **1995**, *270*, 1639.
(17) Fuhrer, A.; Luscher, S.; Ihn, T.; Heinzel, T.; Ensslin, K.; Wegscheider, W.; Bichler, M. *Nature* **2001**, *413*, 822.
(18) Delacour, C.; Claudon, J.; Poizat, J.-P.; Pannetier, B.; Bouchiat, V.; Lamaestre, R. E.; Villegier, J. C.; Tarkhov, M.; Korneev, A.; Voronov, B.; Gol'tsman, G. *Appl. Phys. Lett.* **2007**, *90*, 191116.
(19) After submmission of this work, we became aware of a similar work by Li and co-workers also proposing the fabrication of gas sensors via LAO: Li, Z.; Wu, M.; Liu, T.; Wu, C.; Jiao, Z.; Zhao, B. *Ultramicroscopy* **2008**, *108*, 1334.

10.1021/la803105f CCC: $40.75
Published on Web 12/11/2008

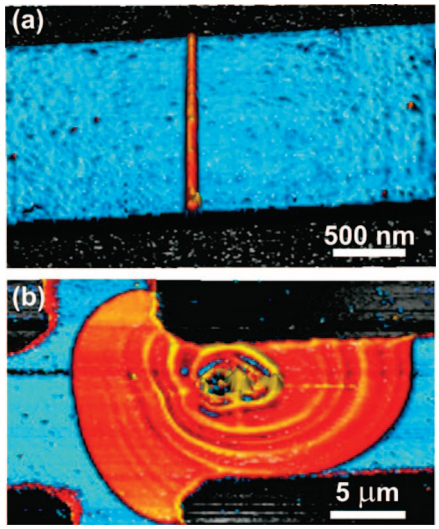

Figure 1. AFM images revealing the topography (three-dimensional rendering) of typical nanosensor (a) and microsensor (b) produced via slow (a) and fast (b) LAO routes. (a) A nanowire-type TiO_x region (orange) is formed in the 8 nm-thick Ti track (blue), which partially covers the SiO_x substrate (black). (b) A round-shaped MoO_x region (orange-yellow) is formed in the 20 nm-thick Mo track (blue), which partially covers the SiO_x substrate (black).

Two distinct LAO routes can be employed in the second fabrication step: a slow (conventional) or a fast (unusual) process, enabling the definition of nano- or micron-size metal oxide regions, respectively, which will constitute the active region of the sensor. In this work, each LAO route is SPM-based, i.e., the metal oxide is formed through an electrochemical reaction in the region beneath a properly biased AFM tip.[13−15,19−21] In the slow process, conventional tip biases V_T ($|V_T| \leq 30$ V) and scan speeds (100 nm/s $\leq V \leq 10$ μm/s) allow a high control of both size and geometry of the oxide pattern, producing wire-type active regions down to the nanoscale (a few tens of nanometers wide and several hundreds of nanometers long).[13−15,20] On the other hand, in the fast process, the AFM tip is kept stationary on top of any given region of the metal track (no accurate positioning is needed), and a high voltage bias pulse ($t \leq 120$ s, $|V_T| \geq 50$ V) is applied. This process produces round-shaped oxide regions, which, depending on pulse duration and magnitude, have a radius ranging from hundreds of nanometers to a few microns.

In the present work, both AFM imaging and LAO is accomplished using an NT-MDT Solver Pro SPM operating in intermittent contact mode. Silicon probes, coated with conductive diamond-like carbon (DCP11 series, from NT-MDT, with a resonant frequency of ~150kHz and a force constant of ~5N/m), are employed because of their higher conductivity and greater resistance to oxidation than bare silicon probes. In order to optimize it, the LAO process is performed under a relative humidity of 60%, controlled by a homemade system. Each sensor is tested in a homemade chamber, where sample temperature can be varied from room temperature to 400 °C, equipped with mass flux control valves. During each measurement, both the total gas flux and temperature are kept constant. The sensing activity of a sensor is detected via current measurements using a Keithley electrometer model 6517A.

Results and Discussion

Figure 1a (b) shows a topographic AFM image of a typical nano- (micro-) sensor made out of a Ti/TiO_x (Mo/MoO_x) system using the slow LAO route at $V = 1$ μm/s and $V_T = 10$ V (fast LAO route with $V_T = 60$ V for ~2s). In both figures, a thin metal track (8 nm Ti [Figure 1a] and 20 nm Mo [Figure 1b]) is visible (in blue) atop the SiO_x substrate (in black). The nanowire-type region in Figure 1a and the round-shaped region in Figure 1b (both in orange-yellow colors) are the TiO_x and MoO_x active regions of the sensor, respectively. As expected, the slow LAO route produces a uniform nanoscale oxide line (12 nm thick, ~60 nm wide, and ~1.5 μm long) crossing the entire width of the metal track,[20,21] whereas the fast LAO route yields a less uniform oxide (an average thickness around 60 nm is found for the MoO_x region). It is interesting to note in Figure 1b the shockwave-like morphology of this Mo oxide, with a hole in its "epicenter", which represents the standing position of the AFM tip during the bias pulse application. Such morphology, observed only for a few cases where high bias is applied, is probably related to a variation of the water meniscus during the fast oxidation. Making the oxidation process slower (lowering bias and/or lowering ambient humidity) prevents the formation of this shockwave-like morphology. Nevertheless, such morphological variation has no significant effect on device performance, i.e., similar sized devices (smooth and shockwave-like) present similar responses (data not shown).

After the oxidation process, which produces the active region of the sensor, an immediate question arises regarding the nature of such oxide. In other words, what is the oxide stoichiometry, or in what valence state is the metal in the oxide? Because of the small oxide size and the presence of the precursor metal in the surrounding track, direct measurements via X-ray photoelectron spectroscopy (XPS) did not produce any conclusive results. Nevertheless, an estimation of oxide stoichiometry can be made comparing the thickness of the oxide and metal layers.[20] For the majority of devices produced in this work, the thickness ratio between the TiO_x and Ti layers is 1.55 ± 0.05, which, according to the work of Dengfeng and colleagues, indicates an approximate $TiO_{1.4}$ oxide stoichiometry.[20] For the Mo oxide, the MoO_x/Mo ratio is 3.2 ± 0.1, which suggests an exact MoO_3 stoichiometry. Such Mo oxide phase should be water soluble, which is indeed observed experimentally.

Following fabrication, the response of each sensor is analyzed under H_2 (reducing) and CO_2 (oxidizing) test gases in a commercial N_2 (dry air) atmosphere at constant flux and three different temperatures. At each temperature, the system is allowed to stabilize until a constant baseline (current through the device) is obtained. Typical values of current flowing through the devices range from tens of picoamperes up to a few microamperes at 1 V of applied bias. During all experiments, each test gas pulse is 400 s long, its respective washing time is 800 s long, and, thus, only the test gas concentration varies. The relative sensitivity S for a given concentration of the test gas, also labeled as the response of the sensor, is computed simply as $S = I/I_0$, where I_0 (I) is the current through the device under N_2 (test gas) flux.

Figure 2a,b respectively shows the response of the TiO_x nanosensor (Figure 1a) to H_2 at ppm concentration levels and the response of the MoO_x microsensor (Figure 1b) to 8% of CO_2 at different temperatures.[22] In Figure 2a, the TiO_x nanosensor is kept at 220 °C while H_2 pulses (black line) are introduced in the test chamber and the device relative current I/I_0 is monitored (red line). It is easy to see in Figure 2a the sensing response of this nanosensor: its relative current I/I_0 increases upon H_2 pulse. Moreover, its sensitivity also increases with H_2 concentration. It is worth noting the significant sensitivity (~33%), which is already obtained even for the lowest H_2 concentration used in this work (360 ppm). Figure 2b also undoubtfully demonstrates the sensing capability of the MoO_x microsensor fabricated with

(20) Dengfeng, K.; Qinggang, L.; Weilian, G.; Shilin, Z.; Xiaotang, H. *Ultramicroscopy* **2005**, *105*, 111.
(21) Chiu, F. C.; Fan, S. K.; Tai, K. C.; Lee, J. Y.; Chou, Y. C. *Appl. Phys. Lett.* **2005**, *87*, 243506.

(22) See Supporting Information.

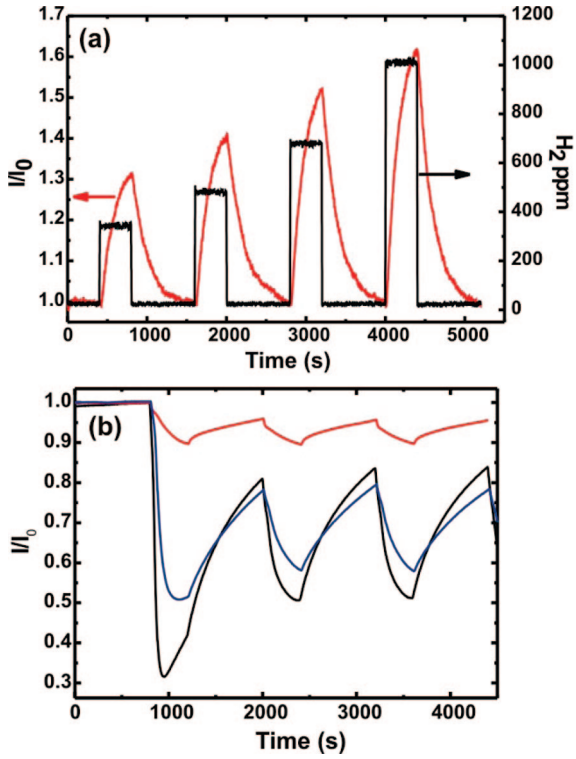

Figure 2. Sensing response of nanosensors and microsensors to test gases. (a) Relative current variation I/I_0 of the TiO_x nanosensor with time (red line) as a response to H_2 concentration (black line), which varies from 360 ppm up to 1000 ppm (in commercial N_2 (dry air) atmosphere). (b) Relative current variation I/I_0 of the MoO_x microsensor with time to 8% of CO_2 square pulses (in commercial N_2 (dry air) atmosphere) as a response to temperature variation (237 °C - red line; 284 °C - blue line; and 329 °C - black line).

the fast LAO route. Its sensitivity to CO_2 is a direct function of temperature, increasing with temperature by up to ~50% to 329 °C. Such behavior, though not universal for any test gas, has been observed for macroscopic Mo oxide sensors under some test gases, such as NH_3 and H_2.[23] It should be stressed that both TiO_x and MoO_x sensors work with both test gases (H_2 and CO_2) under different concentrations,[22] although TiO_x sensors show a systematically larger sensitivity when compared to MoO_x sensors at the same conditions, regardless of the LAO route employed in their fabrication.

The sensing properties of this class of devices are based on physical/chemical interactions between the semiconducting metal oxide and the gases in its surrounding atmosphere, which cause a change in the overall system electrical resistance, due to a charge transfer between the adsorbate and the adsorbent.[1−3,24] This charge transfer directly affects the semiconductor conductivity and can also change the barrier junction metal/oxide/metal.[1−3,24] Therefore, for an n-type material in an oxidizing atmosphere, such as CO_2 gas, the reaction of oxygen atoms with the TiO_x surface captures electrons, hence dropping its conductivity.[22] Likewise, such a material, in a reducing atmosphere, such as H_2 gas, must increase its conductivity, as observed in Figure 2a. Therefore, the TiO_x nanosensor responses to both reducing and oxidizing atmospheres corroborate the results of Chiu and co-workers, which shows that TiO_x grown via LAO is an n-type semiconductor.[21] However, the observed responses

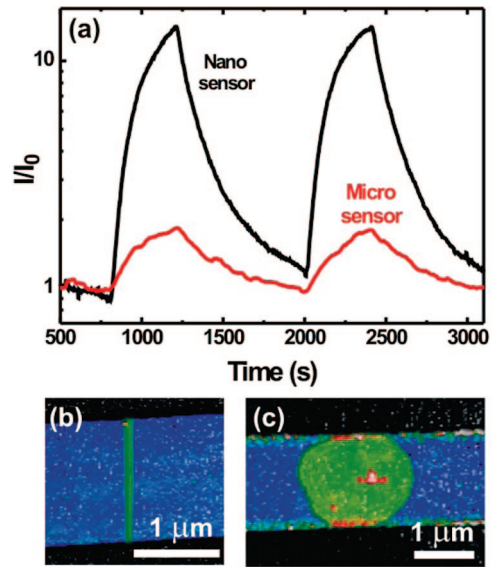

Figure 3. Comparison of the sensing response of a TiO_x nanosensor and microsensor. (a) Relative current variation I/I_0 for both a nanosensor (black line) and microsensor (red line) as a response to 1.5% H_2 concentration at 190 °C. (b,c) AFM topographic images of the nanosensor and microsensor characterized in panel a, respectively.

of MoO_x sensors to both reducing and oxidizing atmospheres are not easily assigned to either pure n-type or p-type semiconductor.[22] Actually, these sensors seem to behave as n-type material when in contact with oxidizing atmosphere, and as p-type when in contact with reducing atmospheres. Such behavior could be associated to p-n-type transitions, which are reported to occur in some resistive-type sensors.[24] Nevertheless, a detailed analysis of the MoO_x sensing mechanism is out of the scope of the present work and is considered a natural step forward of this present investigation.

A question that naturally arises from the results in Figures 1 and 2 is a direct comparison between the sensitivities of a nanosensor and a microsensor under the same conditions. Therefore, TiO_x and MoO_x nanosensors and microsensors were fabricated using the slow and fast oxidation processes, respectively. Some microsensors were also fabricated using the slow process via a sequential oxidation of adjacent lines.[22] The results for MoO_x sensors and TiO_x sensors differ significantly. For MoO_x sensors, the sensitivity is approximately constant, regardless of the sensor size (nano- or micron-scale) or the fabrication method (slow or fast). On the other hand, the sensitivity of TiO_x sensors has a strong dependence on their size scale. Figure 3 shows a direct comparison between a TiO_x nanosensor and a TiO_x microsensor. In Figure 3a, a plot of relative current variation I/I_0 as a function of time shows the different sensitivities of a nanosensor (black line) and a microsensor (red line) under the same conditions ($T = 190$ °C and 1.5% H_2 concentration). Figure 3b,c shows topographic AFM images of the sensors used to produce the data in Figure 3a (Ti track thickness: 11nm; TiO_x active region average thickness: 17nm; nanosensor: slow oxidation; microsensor: fast oxidation). It is clear in Figure 3 that there is an almost 10-fold increase in sensor sensitivity from the micron- to the nanoscale. It is important to stress that this is indeed a size effect and is not related to eventually different Ti oxides on the nano- and microsensor (grown during the respective slow and fast oxidation processes). Micron-scale TiO_x sensors were also fabricated with the slow oxidation process, and the results reproduce those in Figure 3. Therefore, there should be another reason for all the observed results (no size

(23) Mutschall, D.; Holzner, K.; Obermeier, E. *Sens. Actuators, B* **1996**, *35*, 320.
(24) Prasad, A. K.; Kubinski, D. J.; Gouma, P. I. *Sens. Actuators, B* **2003**, *93*, 25.

dependence for MoO_x sensors and significant size dependence for TiO_x sensors).

A possible explanation comes from the working principle of resistive gas sensors, where any given sensor can be viewed as a set of series resistors.[1−3,10−12] Defining R_I as the resistor associated to the semiconductor−metal interface and R_S as the resistor associated to the semiconductor (oxide) surface, then, for a bias V, the current I through the device is controlled by both R_I and R_S ($I = V/(R_I + R_S)$).[1−3,10−12] The value of R_I is approximately size independent, as the semiconductor−metal interface is similar for both nano- and microsensors. On the other hand, it is intuitive to see that the value of R_S increases as the device size increases. When gas species are adsorbed onto a given sensor, the values of R_I and R_S change, but, frequently, by different amounts. For such a sensor, the current I is defined by the total resistance, and the gas sensibility I/I_0 is defined by the total resistance variation under gas exposure. Now, suppose, for the TiO_x case, that R_I shows a large variation upon gas exposure, whereas R_S presents a much smaller variation. Initially, at the nanoscale, R_I and R_S might be similar, and the large variation of R_I causes a large current variation, leading to a good sensitivity. However, as size increases toward the microscale, R_S increases substantially and, eventually, determines the current through the device. Any variations on R_I will have a much smaller effect on the current, resulting in a smaller gas sensitivity I/I_0, as observed. On the other hand, suppose, for the MoO_x case, that R_I varies only slightly under gas exposure, whereas R_S presents a larger variation, and $R_I < R_S$. Therefore, the sensing response of a MoO_x sensor is governed by R_S variation only. As the sensor size increases, from nano- to microscale, R_S increases (the current decreases), but since the relative variation $\Delta R_S/R_S$ is fixed, the sensitivity I/I_0 remains approximately constant.

The above analysis is in agreement with the experimental data, thus suggesting two different working principles for TiO_x and MoO_x sensors. While the metal/oxide interface is the most sensitive region of a TiO_x sensor, for a MoO_x sensor, the oxide surface is the most sensitive region.

The results shown in Figures 1, 2, and 3 demonstrate the accomplishment of the novel sensor fabrication method proposed in this work. Nano- and micron-scale sensors show suitable sensitivities and response/recovering times. Although this might be scientifically important, it is not the only achievement of this method. The direct fabrication of the sensor active region in a metallic track, with nano- or micron-scale resolution, also bears potential technological advances. The fact that the sensors (active regions) are "born" electrically connected down to the nanoscale eliminates many time-consuming steps, which are typical to nanowire-based sensor fabrication, such as localization, manipulation and contacting of the active region (nanowire). Indeed, the process employing the fast LAO route could be easily implemented into industrial microfabrication processes. It does not require nanometer-precision during tip positioning and scanning, as the slow LAO route does, nor is it as time-consuming. Its features, such as no need of tip movement nor accurate positioning (micron-scale accuracy, achievable with optical microscopy, is enough), are right within the current capabilities of any microfabrication industry. Moreover, it is easy to see that this method could be straightforwardly integrated into a complex semiconductor device microfabrication process, creating further possibilities in the design of smart, or intelligent, devices.

Conclusion

In conclusion, this work demonstrates a new methodology of sensor fabrication down to the nanoscale that is based on photolithography and LAO techniques. Two different metal oxides (MoO_x and TiO_x) are employed as proof-of-concept materials, producing sensors with suitable response and sensitivities down to low concentrations of both reducing and oxidizing gases. In principle, this methodology, including both slow and fast LAO routes, could be applied to any desired metal or metal alloys, further extending sensing possibilities of designed nano- and microdevices. Finally, this novel sensor design and fabrication concept is proposed in a way that it could be readily implemented in conventional industrial microfabrication processes.

Acknowledgment. The authors acknowledge financial support from CNPq, Fapemig, Instituto do Milênio de Nanociências and Nanotecnologia/MCT, and CT-Petro/MCT. B.S.A., G.V.S., A.-M.B.G., and D.C.B.A. are thankful to CNPq and CAPES for their scholarships.

Supporting Information Available: A complete set of test data, showing the response of each sensor in Figure 1 to both CO_2 and H_2 gases in several concentrations at different temperatures, and some different possibilities of active region (sensor) fabrication. This material is available free of charge via the Internet at http://pubs.acs.org.

LA803105F